PERGAMON

Planetary and Space Science 49 (2001) 313–318

Planetary and Space Science

www.elsevier.nl/locate/planspasci

High-latitude radiation and resonant enhancements of the Jovian synchrotron emissions

Ilan Roth[a,*], Reuven Ramaty[b]

[a] *Space Sciences Laboratory, University of California, Berkeley, CA 94720, USA*
[b] *Laboratory for High Energy Astrophysics, Goddard Space Flight Center, Greenbelt, MD 20771, USA*

Received 16 November 1999; received in revised form 12 May 2000; accepted 15 May 2000

Abstract

A model describing (1) short time scale increases in Jovian synchrotron radiation and (2) emissions from high Jovian latitudes is presented. In the present model resonant interaction between oblique whistler waves and relativistic electrons diffuses the energy and the pitch angle of electrons which bounce along the Jovian magnetic field. The resonant interaction violates the first two adiabatic invariants and the energy diffusion results in hardening of the electron spectrum and in intensification of the synchrotron radiation. This model complements the radial diffusion process which (a) violates the third adiabatic invariant of a seed population via interaction with low-frequency magnetospheric oscillations and (b) increases the flux of energetic electrons at low L-shells over long time scales by conserving the first adiabatic invariant. The high-latitude emissions indicate also acceleration of bouncing electrons and radiation in the region of the strongest magnetic field. The seed particles and whistler waves determine the form of the electron distribution tail. This tail enhances the high-latitude synchrotron radiation observed at Earth. The resulting emissivities of the nonthermal radio waves in the ordinary/extraordinary modes of propagation, the polarization and the intensity spectrum observed at Earth due to these high-energy populations are calculated.

1. Introduction

Since the discovery of radio emission from Jupiter (Burke and Franklin, 1955) it is widely accepted that the Jovian radio waves can be classified according to their frequency as decametric (<40 MHz) due to cyclotron emissions and decimetric (0.1–15 GHz) due to synchrotron radiation, with a thermal component at its higher end. The Jovian synchrotron radiation is seen at Earth above the galactic noise level due to its strong magnetic field (4.28 G at the equator) and a sufficiently intense flux of energetic electrons ($>$few MeV). This radiation, known for a long time (e.g. Radhakrishnan and Roberts, 1960; Morris and Berge, 1962) was used in determining the inclination of the magnetic dipole field with respect to the rotational axis, as well as the magnitude of the multipole correction to the field (Warwick, 1963). The temporal increases in the Jovian synchrotron radiation detectable at Earth, which are still controversial (Gerard, 1976) are probably due to enhancement of fluxes of relativistic electrons at low L-values (equatorial distance in radial units). High-resolution radio images from the very large array indicate emissions at high latitudes (de Pater et al., 1997). Some of the scientific questions which are addressed in the present paper concerning the triggers of these enhancements are related to their sites, the time scales involved in the increase of the electron fluxes and the energization mechanisms of relativistic electrons. Jovian synchrotron radiation which emerges around $L = 1.5$ exhibits (1) long-term variations (over periods of months) due to changes in the solar wind conditions, which modify the electron phase-space density at the outer boundary, resulting in diffusive heating of the equatorial electrons, and (2) possibly much shorter (days) increases due to other processes. Long-term changes in the synchrotron radiation were correlated with an increase/decrease in the dynamic solar wind (SW) pressure (Bolton et al., 1989) resulting in a synchrotron radiation lag time of several months. Therefore, it is believed that an increase in the dynamic pressure of SW modifies the boundary conditions at the outer Jovian magnetosphere by an enhanced injection of the seed population, and the slow diffusion due to the ultra-low perturbations at high L or upper atmospheric turbulence at low L shells transports the electrons towards the planet and enhances the flux of relativistic electrons at the region of the synchrotron

* Corresponding author. Tel.: +1-510-642-1327; fax: +1-510-643-8302.
E-mail address: ilan@ssl.berkeley.edu (I. Roth).

0032-0633/01/$ - see front matter
PII: S0032-0633(00)00152-5

radiation emission (de Pater and Goertz, 1990, 1994). Short-term increase in the synchrotron radiation has an unknown source (except in the catastrophic impacts, like SL9). Numerical calculations of electron radial diffusion in the Jovian magnetosphere have shown (de Pater and Goertz, 1994) that it is impossible to trigger short-term enhancements in radio emissions by increases in the phase density at some outer boundary, as prescribed by enhanced SW pulses. Short-term variability are due, presumably, to in-situ processes in the inner magnetosphere. Additionally, radio emissions at high latitudes indicate energization of bouncing electrons with equatorially small pitch angles.

In contrast to the L-diffusion which may explain the slow increase in energetic electron distributions mainly in the equatorial plane via violating the third adiabatic invariant, in this paper the local interaction (on a given L-shell) of oblique whistler waves with energetic electrons which bounce along the magnetic field is presented. These whistler waves propagate at Jovian magnetosphere, acquire significant oblique wavenumbers along their paths due to the changing magnetic field and density profile (e.g. Thorne and Horne, 1994) and therefore are able to interact resonantly at several regular and anomalous gyroharmonic resonances. The interaction at higher and anomalous gyroharmonics is particularly efficient for relativistic particles with gyroradii of the order of the whistler wavelengths. This interaction violates the first and the second adiabatic invariants, and the resulting diffusion in pitch angle and in energy results in hardening in the spectrum of the relativistic electrons over time scales much shorter than those related to the L-diffusion. The interaction with the oblique whistler waves may also explain the observation of a synchrotron radiation at high latitudes, since most of the multiple harmonic resonances occur off the equatorial plane and the emission is intensified at stronger magnetic field. With the help of a particle code in a simplified geometry, the effects of whistler waves on the relativistic electrons is investigated. The characteristics of synchrotron radiation due to the resulting enhanced tail of the distribution function at given magnetic field is calculated.

2. Interaction with Jovian whistlers

Lightnings and substorms are sources of whistler waves in the Earth's magnetosphere. Lightnings were reported numerous times at Jovian magnetosphere, mainly at the inner edge of the Io torus (Gurnett et al., 1979; Kurth et al., 1985), and whistler waves were observed at all the encounters of satellites with the outer planets. The typical dispersion of the whistlers allowed to model the total electron concentration along their propagation paths (Gurnett et al., 1981), the proton densities and anisotropies in the inner magnetosphere (Crary et al., 1996) and it indicated that their source location are in Jovian atmosphere (Kurth et al., 1985; Wang et al., 1998). Jovian measurements indicate a possible correlation between whistler enhancements and increase in the intensity of ~ 100 keV electrons (Williams, 1999), similarly to substorm characteristics at the Earth, where the injected electrons excite whistler waves due to the velocity dispersion during their grad-B drift (Smith et al., 1996). Additionally, an analysis of Galileo data suggests the existence of dynamic processes analogous to terrestrial substorms, together with enhanced auroral emissions, magnetic field distortions and injection of energetic particles (Woch et al., 2000).

When a whistler wave propagates obliquely to an inhomogenous magnetic field, it can interact with energetic electrons through Landau ($n = 0$), cyclotron ($n = 1, -1$), and higher harmonic resonant interactions when the Doppler-shifted wave frequency equals any (positive or negative) integer multiple of the relativistic gyrofrequency. This process involves resonant interaction with electrons bouncing and gyrating along the inhomogeneous dipole magnetic field, $\omega - k_{||}v_{||} - n\Omega/\gamma \sim 0$, where the wave is characterized by its frequency ω and parallel wavenumber $k_{||}$ and the resonating electron by its parallel velocity $v_{||}$, local gyrofrequency Ω and the relativistic factor γ, while the integer n denotes the harmonic of the cyclotron interaction. The gyroradius of an energetic electron may be the order of or greater than the perpendicular wavelength, hence along the electron bounce trajectory many cyclotron harmonics can contribute to the resonant interaction, which breaks down the first two adiabatic invariants. The irreversible changes in the adiabatic invariant depend on the relative phase between the wave and the electron, and successive resonances result in electrons undergoing an independent random walk in energy and pitch angle. This stochastic interaction operates on the bounce time scale, hence is faster in energy diffusion than the equatorial L-shell diffusion. Therefore, this local heating process may contribute significantly to a rapid formation of a high-energy tail on the electron distribution.

3. Simulation model

Energetic electrons which bounce along the Jovian magnetic field and encounter the resonant waves may experience irreversible changes in their adiabatic invariants. For obliquely propagating whistlers the intensity of the interaction between the gyrating electron and the wave depends also on the ratio between the perpendicular wavelength and the gyroradius. Electrons with gyroradius of the order of the perpendicular wavenumber which propagate to high latitudes interact with numerous harmonics of the cyclotron resonance. The interaction between the whistler waves and the energetic electrons is simulated along an inhomogeneous model magnetic field in Cartesian coordinates,

$$B(x, y, z) \sim B_{\mathrm{eq}}[1 + z(z\hat{z} - x\hat{x} - y\hat{y})/D^2], \tag{1}$$

where z denotes the coordinate along the field axis (increases with latitude), $\hat{z}, \hat{x}, \hat{y}$ are the appropriate unit vectors, R is the Jovian radius, $D \sim RL$ and $B_{\mathrm{eq}} = B_{\mathrm{o}}/L^3$ is the equatorial

field on a given L-shell. Eq. (1) satisfies $\mathrm{div}\, B = 0$, includes the effect of mirror force and implies explicitly a bounce motion along the magnetic field.

The propagation of the wave is not considered explicitly, since we are interested in diffusive properties of the resonant interaction between waves and bouncing electrons. Previous investigations indicated unducted wave propagation with large oblique wavenumbers and accessibility of whistlers to regions far from their source (Church and Thorne, 1983; Horne, 1989; Wang et al., 1998). Energetic electron with a large equatorial parallel velocity, which bounces along the inhomogeneous magnetic field and satisfies the resonance conditions with $\omega \ll \Omega$, encounters the resonances which do not depend sensitively on the range of whistler frequencies, hence for the sake of simplicity we consider here interaction between coherent waves and bouncing electrons at different resonances and varying latitudes. The waves are modeled by propagating electromagnetic disturbances whose properties are modified along the axis of propagation due to changing plasma parameters (mainly the strength of the magnetic field). The wave electric field is given by $[E_x \cos\psi, E_y \sin\psi, E_z \cos\psi]$ with $\psi = [\int \mathbf{k}(\varepsilon z)\, \mathrm{d}\mathbf{x} - \omega t + \phi]$, where ϕ is an arbitrary phase and the ε functional dependence emphasizes the slowly changing wavenumber $\mathbf{k} = (k \sin\theta, 0, k \cos\theta)$ along the electron trajectory. The refractive index, the wavenumber and the amplitudes of the electric/magnetic field components are recalculated each time step from the cold dispersion relation. Since energetic electrons consist of a very small density vs. the cold distribution, the cold approximation is justified for the dispersion relation. Explicitly, the square of the refractive index c^2k^2/ω^2 is given by $[B - (B^2 - 4AC)^{0.5}]/2A$, with

$$A = \varepsilon_1 \sin^2\theta + \varepsilon_3 \cos^2\theta,$$
$$B = \varepsilon_1\varepsilon_3 + \varepsilon_1 A - \varepsilon_2^2 \sin^2\theta,$$
$$C = \varepsilon_3(\varepsilon_1^2 - \varepsilon_2^2), \qquad (2)$$

where ε_i denote the standard components of the dielectric tensor (e.g. Krall and Trivelpiece, 1986). Local expansion of $\cos\psi$ with the help of Bessel functions J_n gives terms like $J_n(k_\perp v_\perp \gamma/\Omega)\cos(k_{||}v_{||} - \omega + n\Omega/\gamma)t$, indicating the importance of resonances for an effective interaction, when the argument of cos is changing very slowly.

For each particle the dynamical system is propagated in time as a six-dimensional vector which describes the phase space $\mathbf{X} = (x, y, z, v_x, v_y, v_z)$. The set of the coupled equations

$$\dot{\mathbf{X}} = \mathbf{G}(\mathbf{X}), \qquad (3)$$

where $\mathbf{G}$ propagates the phase space dynamics via the prescribed electromagnetic fields (external constant magnetic field and electric/magnetic wave field obtained from the dispersion relation) is solved with an adaptive time step. Due to the structure of the electromagnetic forces, Eq. (3) describes an autonomous (no time dependence on the r.h.s.) and conservative (volume preserving, i.e. $\nabla\mathbf{G} = 0$) system.

The simulations employ a fourth-order Runge–Kutta method with an adaptive time step (Press et al., 1986). Initial wave number propagation angle is specified as well as the three electron velocities and positions. The variables which describe the evolution of the system include particle phase space and wave phase ψ. The relativistic equation of motion (Eq. (3)) is integrated together with the wave phase and we focus on the diffusion due to the nonadiabatic changes at the resonances.

4. Diffusive electron trajectories

In the simulations we choose a range of parameters: electric field amplitude of 0.1–1 mV/m, scale length of background magnetic field $D = 60\,000$–$120\,000$ km, perpendicular wavenumber $k_\perp = 1$–10 km^{-1}, equatorial magnetic field $B_{\mathrm{eq}} = 1.5 \times 10^{-3}$–$2.0 \times 10^{-2}$ G, density 1–10 cm^{-3}, wave frequency $\omega = 1$–10 kHz, and we vary the initial energy, pitch angle, gyrophase and propagation direction of the whistler wave. Fig. 1 describes (a) the temporal evolution of the kinetic energy $W = mc^2(\gamma - 1)$, (b) the first adiabatic invariant μ, (c) the equatorial pitch angle α (related to the second adiabatic invariant), over a few bounce periods (6.0 s) and the few first electron resonance crossings. μ is calculated by its lowest-order approximation at the electron position: $p_\perp^2/B(\mathbf{x})$, while α is calculated by adiabatically projecting the instantaneous pitch angle to the equator ($z = 0$) with the help of the momenta $(p_z, p_\perp)$: $\alpha = tg^{-1}[p_\perp/[p_\perp^2(z/D)^2 + p_z^2(1 + (z/D)^2)]^{1/2}]$. Fig. 1(d) shows the calculated normalized resonance criterion $v(t) = [\gamma(t)\omega - k_{||}(z)p_{||}(t)]/\Omega(\mathbf{x}(t))$. Here the equatorial magnetic field is 0.01 G, $E = 1$ mV/m is borrowed from the terrestrial values, proportional to the stronger magnetic field and $k_\perp = 10$ km^{-1} is a value which allows for an interaction with many harmonics. The pitch angle was chosen as some average value. $\Omega[\mathbf{x}(t)] = qB[\varepsilon\mathbf{x}(t)]/mc$ denotes the nonrelativistic gyrofrequency which changes along particle trajectory and γ is the relativistic factor. Between resonances ($v(t)$ not too close to an integer n) the electron moves adiabatically, i.e. both adiabatic invariants are constant as seen in segments of Fig. 1, but when it crosses a resonant region (v approaches an integer n), an irreversible change in energy, in first adiabatic invariant and in equatorial pitch angle may occur. One observes that the electron performs a random walk in all quantities. Because the resonant interactions include a variety of positive and negative values of n, changes in energy and in pitch angle are not correlated. Additionally, in contrast to the energy and the pitch angle, the adiabatic invariant is not affected by the $n = 0$ resonance.

The irreversible changes in μ, α and in W at resonance crossings can be positive or negative and depend on the relative phase between the wave and the bouncing electron. Two electrons with the same initial energy but not the same pitch angles mirror at different latitudes resulting in interaction with different wave resonances, and because they differ in gyroradii the strength of the interaction will vary too.

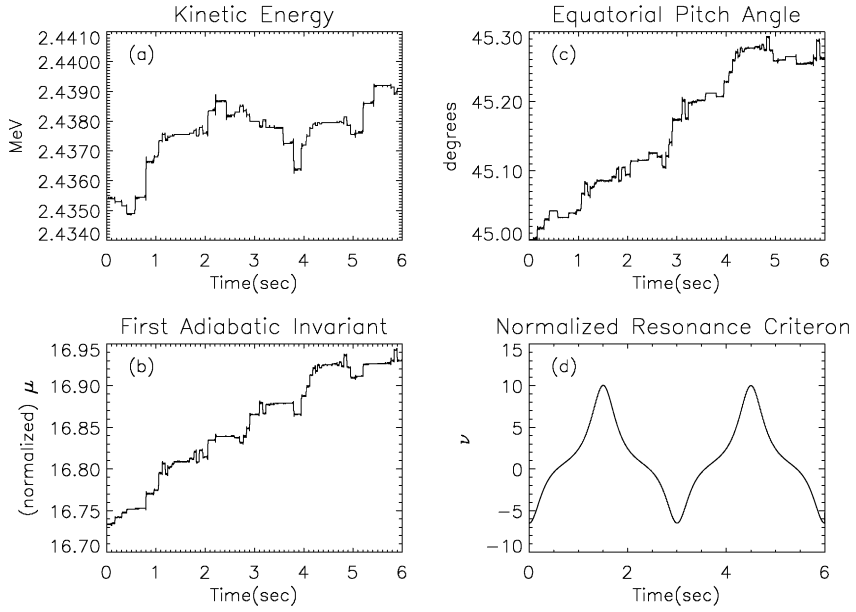

Fig. 1. Temporal evolution of (a) relativistic kinetic energy W, (b) first adiabatic invariant μ, (c) equatorial pitch angle α and (d) resonance criterion v. $B_{eq} = 0.01$, $D = 100\,000$ km, $E_o = 1$ mV/m, $k_\perp = 10$ km^{-1}, density $= 10$ cm^{-3}. Initial pitch angle $\alpha_o = 45^\circ$, initial gyrophase $\delta_o = 45^\circ$.

However, since the changes in the adiabatic invariants depend on the (random) phases at the entry into the resonant region, the successive resonant interactions create a stochastic process. Since the distribution function of the seed electrons generally decreases with energy, the main manifestation of the diffusion process involves expansion into the lower-density region of the phase space and therefore may be seen as an increased flux at higher energies. An analysis of resonant dispersion curves for parallel propagating whistler waves showed that the diffusion results in a κ distribution with a significant tail (Ma and Summers, 1999). For general oblique propagation the different resonances between electrons and whistler waves are not correlated, hence their stochastic interaction will result in tail enhancement too. Therefore, pulses of whistler waves can significantly contribute to the increase in the fluxes of Jovian relativistic electrons on time scales which are several orders of magnitude faster than radial diffusion due to ultra-low-frequency waves, which are usually considered as a source of an electron diffusion and an increase of electron energies. The increased tail at the electron distribution function will be used to calculate the enhanced radio emission.

5. Radio emissions

The theory of radio emission by relativistic electrons is believed to account for many observed emissions from a variety of cosmic sources (e.g. Ginzburg and Syrovatskii, 1964). The full description of the synchrotron emission in the presence of strong magnetic field includes the effects of ambient medium and reabsorption by the radiating electrons themselves (e.g. Ramaty, 1969; Ramaty et al., 1994). In the presence of magnetized plasma the radiation may propagate at different modes (ordinary O and extraordinary X) and for a Lorentz factor γ below the plasma-to-gyrofrequency ratio, the emissions at low frequencies are substantially suppressed (Razin effect). The reabsorption affects the wave power spectrum and modifies the polarization of the resultant radiation.

Figs. 2a, b and c, d show the gyrosynchrotron emissivity of the radio emission and the absorption coefficients, respectively, as a function of frequency (in units of the gyrofrequency). The distribution of electrons was taken as a power-law in energy $g(E) = N_o E^{-\alpha}$ with an index $\alpha = 2.5$, while the angle between the magnetic field and the line of sight Θ was taken arbitrarily as 45°. The magnetic field is assumed constant at $B = 1$ G, i.e. the calculations describe, for example, emission from a high-latitude, low-L region. The absolute values of the radiation intensity are proportional to the electron density N_o and to the size of the radio source. Both the emissivities and absorption coefficients are normalized to electron number density $E^{-\alpha}$. The units of emissivity are ergs^{-1} sr^{-1} Hz^{-1} cm^{-3} but since their values depend on the proportionality constant of the relativistic electrons and the size of the source they are presented in normalized units. The source size was taken as a small fraction of the flux tube. The calculations perform a summation of many terms with Bessel functions over both modes of propagation, resulting in oscillatory behavior at the lower part of the spectrum. Above the transition energy of 10 MeV the calculations use the ultrarelativisic approximation (Ginzburg and Syrovatskii, 1965). Since the radiation can be reabsorbed by the plasma the radio emission spectrum is

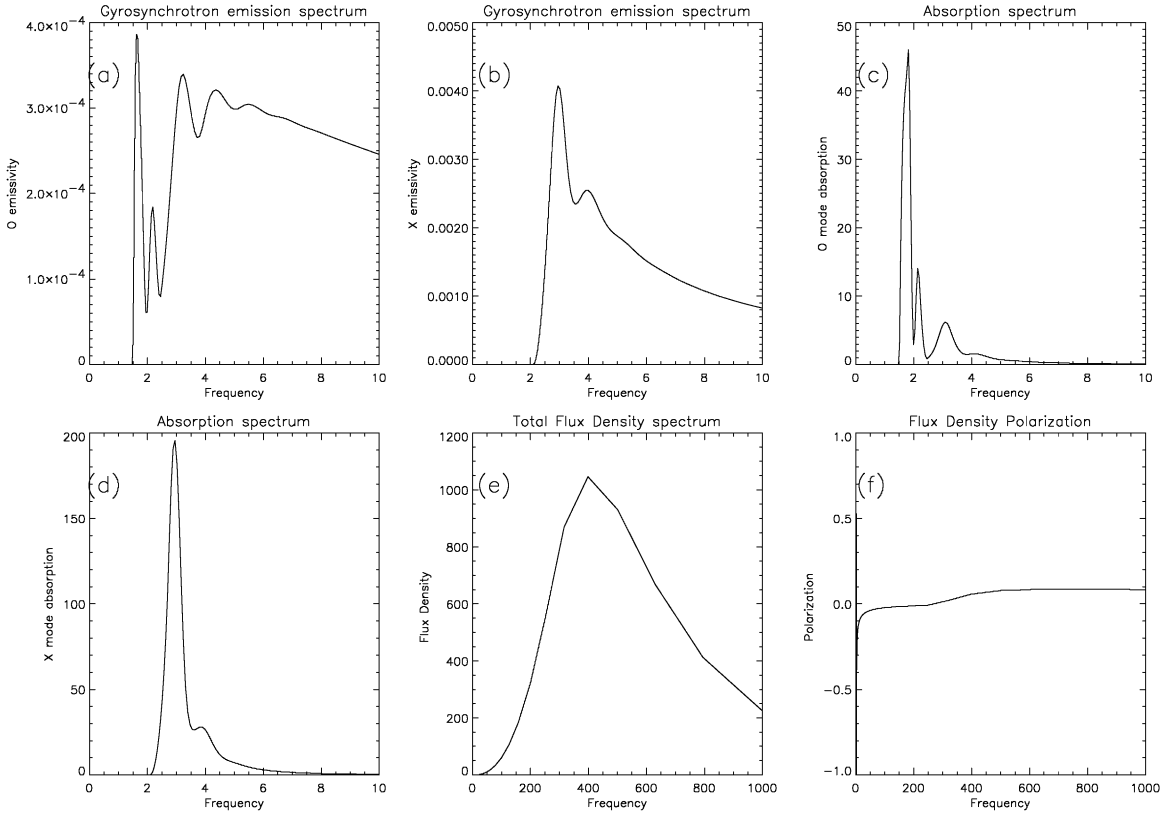

Fig. 2. Radio spectral emission for electron distribution with a power-law $\alpha = 2.5$ and magnetic field $B = 1$ G. (a), (b) O/X emissivities; (c), (d) O/X absorption coefficients; (e) total flux density; (f) polarization. The frequency is given in units of the gyrofrequency. Note the varying spectral range.

significantly different from the spectrum of emissivity. Fig. 2e presents the total flux density spectrum observed at Earth (first Stokes parameter), normalized to the total electron number $g(E)$. One observes that the peak occurs at high harmonic and the spectrum extends to very high harmonics of the gyrofrequency (for $B = 1$ G the value of the highest plotted frequency is 2.8 GHz). Fig. 2f shows the degree of polarization calculated from the flux densities, depicting a departure from zero at low frequencies and slowly changing polarization at higher frequencies.

6. Summary

The emissions of synchrotron radio waves at high Jovian latitudes and increases in the emissions over times scales much shorter than those obtained from radial diffusions are presented by a model which incorporates the interaction between bouncing electrons and whistler waves. Synchrotron emissions require strong magnetic field and relativistic electrons. The resonant interaction of a seed electron population with oblique whistler waves which propagate with group velocities approximately along the inhomogeneous magnetic field lines results in several resonant regions of interaction in one single bounce. These resonances diffuse the electrons in pitch angle and in energy, resulting in hardening of the spectrum at high energies. Similar to terrestrial magnetosphere, Jovian lightnings constitute one of the sources of whistler waves while Jovian substorms may possibly create a seed population of relativistic electrons as well as of whistler waves. The relativistic electrons which were energized during their bounce motion along the dipole Jovian magnetic field by whistlers emit radio waves at all latitudes; since the interaction at higher latitudes with a stronger Jovian magnetic field involves electrons which move slower parallel to the field, those particles will tend to emit more radiation at the higher latitudes. Additionally, one should expect enhancements of radio emission over short times due to an increased level of whistler activity. These enhanced radio waves at high latitudes could be detected at Earth.

Acknowledgements

The authors acknowledge the support by NASA Grants NAG5-6985, NAG5-4898, NAG5-3596, NAG5-3182, and NAG5-8078.

References

Bolton, S.J., Gulkis, S., Klein, H.J., de Pater, I., Thompson, T.J., 1989. Correlation studies between solar-wind parameters and the decimetric radio emission from Jupiter. J. Geophys. Res. 94, 121.

Burke, B.F., Franklin, K.L., 1955. Observations of a variable radio source associated with the planet Jupiter. J. Geophys. Res. 60, 213.

Church, S.R., Thorne, R.M., 1983. On the origin of Plasmaspheric hiss: ray path integrated amplification. J. Geophys. Res. 88, 7941.

Crary, F.J., Beganal, F., Ansher, J.A., Gurnett, D.A., Kurth, W.S., 1996. Anisotropy and proton density in the Io plasma torus derived from whistler wave dispersion. J. Geophys. Res. 101, 2699.

de Pater, I., Goertz, C.K., 1990. Radial diffusion models of energetic electrons and Jupiter's synchrotron radiation 1. Steady state solution. J. Geophys. Res. 95, 39.

de Pater, I., Goertz, C.K., 1994. Radial diffusion models of energetic electrons and Jupiter's synchrotron radiation 2. Time variability. J. Geophys. Res. 99, 2271.

de Pater, I., Schultz, M., Brecht, S.H., 1997. Synchrotron evidence for Amalthea's influence on Jupiter's electron radiation belt. J. Geophys. Res. 102, 22 043.

Gerard, E., 1976. Variation of the radio emission of Jupiter at 21.3 and 6.2 cm wavelength. Astron. Astrophys. 94, 353.

Ginzburg, V.L., Syrovatskii, S.I., 1964. The origin of Cosmic Rays. Macmillan, New York.

Ginzburg, V.L., Syrovatskii, S.I., 1965. Ann. Rev. Astron. Astrophys. 3, 297.

Gurnett, D.A., Scarf, F.L., Kurth, W.S., Shaw, P.R., Poyntier, R.L., 1981. Determination of Jupiter's electron density profile from plasma observations. J. Geophys. Res. 86, 8199.

Gurnett, D.A., Shaw, P.R., Anderson, R.R., Kurth, W.S., 1979. Whistler observed by Voyager 1: lightenings on Jupiter. Geophys. Res. Lett. 6, 511.

Horne, R.B., 1989. Path-integrated growth of electrostatic waves. J. Geophys. Res. 94, 8895.

Krall, N.A., Trivelpiece, A.W., 1986. Principles of Plasma Physics. San Francisco Press, San Francisco.

Kurth, W.S., Strayer, B.D., Gurnett, D.A., Scarf, F.L., 1985. A summary of whistlers observed by Voyager 1 at Jupiter. Icarus 61, 497.

Ma, C., Summers, D., 1999. Formation of power-law energy spectra in space plasmas by stochastic acceleration due to Whistler-mode waves. J. Geophys. Res. 21, 4009.

Morris, D., Berge, G.L., 1962. Measurements of the polarization and angular extent of the decimetric radiation of Jupiter. Astrophys J. 136, 276.

Press, W.H., Flannery, B.P., Teukolsky, S.A., Vetterling, W.T., 1986. Numerical Recipes. Cambridge University Press, Cambridge.

Radhakrishnan, V., Roberts, J.A., 1960. Polarization and angular extent of the 960 Mc/sec radiation from Jupiter. Phys. Rev. Lett. 4, 493.

Ramaty, R., 1969. Gyrosynchrotron emission and absorption in a magnetoactive plasma. Astrophys J. 158, 753.

Ramaty, R., Schwartz, R.A., Enome, S., Nakajima, H., 1994. Gamma-ray and millimeter-wave emissions from the 1991 June X-class solar flare. Astrophys J. 436, 941.

Smith, A.J., Freeman, M.P., Reeves, G.D., 1996. Postmidnight VLF chorus events, a substorm signature observed at the ground near $L = 4$. J. Geophys. Res. 101, 24 641.

Thorne, R.M., Horne, R.B., 1994. Landau damping of magnetospherically reflected whistlers. J. Geophys. Res. 99, 17 249.

Warwick, J.W., 1963. The position and sign of Jupiter magnetic moment. Astrophys. J. 137, 1317.

Williams, D., 1999. MOP Conference, Paris.

Wang, K., Thorne, R.M., Horne, R.B., Kurth, W.S., 1998. Constrains on Jovian plasma properties from a dispersion analysis of unducted whistlers in the warm Io torus. J. Geophys. Res. 103, 14 979.

Woch, J., Krupp, N., Lagg, A., Livi, S., Wilson, B., Williams, D.J., 2000. EGS, Nice.